ELSEVIER

Colloids and Surfaces
A: Physicochemical and Engineering Aspects 193 (2001) 85–96

COLLOIDS AND SURFACES A

www.elsevier.com/locate/colsurfa

Spreading dynamics of liquids and surfactant solutions on partially wettable hydrophobic substrates

Maria von Bahr [a,*], Fredrik Tiberg [a], Vassili Yaminsky [b]

[a] *Institute for Surface Chemistry, Box 5607, SE-114 86 Stockholm, Sweden*
[b] *Department of Applied Mathematics, Research School of Physical Sciences and Engineering, Australian National University, Canberra ACT 0200, Australia*

Received 11 September 2000; accepted 30 April 2001

Abstract

The drop spreading of water and aqueous solutions of ethanol and nonionic surfactant on hydrophobic substrates (alkylsilane treated glass) have been investigated. For the low viscous liquids and solutions, the spreading on the surface of hydrophobic glass rod was also studied and compared to the drop spreading experiment. In both experiments, care was taken to ensure a minimum impact of inertial forces. The results for the aqueous systems show rapid initial spreading processes that abruptly halts after less than 30 ms, as the interfacial tension forces are balanced. In the case of surfactants solutions, this is followed by slower adsorption driven drift towards equilibrium conditions. During the initial spreading phase, the wetting front exhibits $\sim t^{1/2}$ spreading law. Two more viscous liquids, ethylene glycol and glycerol, were also examined and found to show a weaker time-dependence in the whole spreading regime. An $\sim t^{1/10}$ scaling of the drop radius versus time was for these liquids observed in the asymptotic long-time regime. For the surfactant solution, a slow relaxation towards equilibrium was observed following the initial fast spreading phase. The rate-limiting process in this regimes was in the drop spreading experiment found to be surfactant adsorption from the bulk to the expanding liquid–vapour interface, whereas surface diffusion at the liquid–vapour interface appeared rate-determining in the rod experiment. The reason for this is the differences in aspect ratio between relative expansion of the liquid–vapour and solid–liquid interfaces during spreading in the two experiments. In the study of surfactant solution spreading, the importance of surface relaxation prior to contact of the solution and the solid was also pointed out.

Keywords: Drop spreading; Meniscus rise; Partial wetting; Aqueous solutions; Surfactant

1. Introduction

Equilibrium wetting properties of liquids and solutions can be interpreted in terms of the balance of surface tensions,

$$\gamma_{SV} - \gamma_{SL} = \gamma_{LV}\cos\theta, \quad (1)$$

* Corresponding author. Tel.: +46-8-790-9900; fax: +46-8-20-8998.
E-mail address: maria.vonbahr@surfchem.kth.se (M. von Bahr).

0927-7757/01/$ - see front matter
PII: S0927-7757(01)00756-7

a conclusion drawn almost two centuries ago by Thomas Young. Eq. (1) defines the wetting tension as the surface tension difference between the solid–vapour and solid–liquid interfaces ($\gamma_{SV}-\gamma_{SL}$). The definition is done in terms of experimentally accessible quantities: the liquid–vapour surface tension (γ_{LV}) and the contact angle (θ). At first sight, equilibrium wetting seems a rather trivial issue, but in reality it rooms a number of subtle issues of which many to date are not fully clarified, cf. Adamson, de Gennes [1,2]. In the present work, however, we shall concentrate on the dynamics of wetting of liquids and solutions at solid surfaces. The discussion will be mainly based on the wetting tension balance given in Eq. (1).

In the literature, the two principal approaches for describing the dynamics of drop spreading are the hydrodynamic and the molecular kinetic model [3–12]. The main difference between the models is the mode of energy dissipation. In the hydrodynamic model, dissipation is the result of viscous drag within the spreading drop, while the molecular kinetic model emphasizes dissipation due to friction at the three-phase contact line (TCL). According to the hydrodynamic approach, the drop radius and the contact angle should exhibit the following asymptotic time-dependence:

$$r \sim t^{1/10}, \tag{2}$$

and

$$\theta \sim t^{-3/10}, \tag{3}$$

whereas the molecular kinetic theory predict slightly higher scaling coefficients:

$$r \sim t^{1/7}, \tag{4}$$

$$\theta \sim t^{-3/7}. \tag{5}$$

Both theories account fairly well for experimental spreading behaviours observed for viscous fluids. The molecular kinetic theory is clearly unsuited for describing the final stages of complete wetting, while the more rigorous hydrodynamic model tends to be less well suited for the high velocity and high contact angle regime [8]. In line with this reasoning, de Ruijter et al. concluded that the molecular kinetic model should fit data when the system is far from equilibrium while the hydrodynamic model should be applied at long spreading times or closer to equilibrium [9].

Spreading of complex fluids occurs in many industrial applications. Oil recovery, spreading of herbicides, coatings and ink-jet printing are just a few examples of our choice. For many applications, the major problem is to increase the speed and uniformity of wetting. To achieve the rapid spreading of water on surfaces, which often are hydrophobic, surfactants or polymers are added as a technological routine. Surfactants used to enhance spreading and induce hydrophilic transitions complicate the wetting process through time-dependent adsorption phenomena that occur at all the three interfaces. The surfactant adsorption is reflected in the associated changes of the surface tensions. Indeed, adsorption phenomena in their thermodynamic and kinetic aspects can completely dominate both dynamic and equilibrium wetting of surfaces by aqueous solutions. The spreading mechanisms of solutions containing surface-active molecules have been the topic of many experimental and theoretical investigations. Among the results that might be interesting in our context we refer to several recent developments [13–26]. In spite of this sound development, many aspects of spreading of surfactant solutions still remain unresolved.

Furthermore, the impact of the drop is also of great importance in several practical applications, such as spray coating, spray painting, ink-jet printing and delivery of agricultural chemicals. The subject of spreading on drop impact has been reviewed by Rein [27]. A number of different impact scenarios were considered in this work. The initial spreading scenario depends of a balance between viscosity, inertia and capillary/surface tension forces. If the impact energy is fairly large, the inertial term that follows by the kinetic energy transfer dominates the initial spreading phase, whereas the surface tension and gravity become the dominating factors for drop impacting with small kinetic energies. Pasandideh-Fard et al. and Mourougou-Candoni et al. [28–30] have further investigated effects of added surfactants on initial spreading of drops impacting a solid at rather high speeds. It was concluded in

both studies that the initial spreading rate was controlled by inertia largely created by the impact momentum. Moreover, it was shown that surfactants had no detectable effects on the spreading at this initial stage. However, they did influence the subsequent process of 'recoiling' of the droplet. It is further known that for the long-time spreading in quasi-static regimes observed on time scales much larger than milliseconds, adsorption kinetics and dynamic interfacial tensions are the factors that control wetting. An additional factor that strongly influences wetting processes is the surface heterogeneity of the solid substrate, which among other implications may cause contact angle hysteresis.

In this work, we attempt to identify the factors that determine spreading rates in different regimes and to consider the associated mechanisms. In these experiments, we investigated spreading of pure water and aqueous solutions of ethanol and of a non-ionic surfactant (polyethylene glycol alkyl ether $C_{14}E_6$) on hydrophobized glass substrates. We have also done spreading experiments on the same type of substrates, with two more viscous liquids, ethylene glycol and glycerol, to emphasise the role of viscous drag on spreading.

2. Materials and methods

The substrates used in the present study were silica glass plates and rods (2 mm in diameter). They were rendered hydrophobic by treatment with dimetyloctylchlorosilane (Fluka, purity > 97%). Before the substrates were exposed to dimetyloctylchlorosilane vapour for several hours, they were cleaned with dichromic acid, rinsed with Millipore™ water and blown dry. After the hydrophobizing step they were thoroughly rinsed with tetrahydrofuran, ethanol and Millipore™ water.

The drop profiles and meniscus rise were recorded with a videostrobo-microscope. By the use of the stroboscope images could be taken at a frequency of up to 570 Hz, i.e. about each 2 ms, up to ten superimposed images on one videoframe. Some of the experiments were monitored with a high speed Kodak Motion Corder Analyzer SR-1000 camera capable of capturing up to 1000 frames per second. The high speed camera was connected to a digital video recorder DV-CAM DSR-V10P (Sony). The initial and subsequent stages of spreading were studied by analysing the video data using NIH image analysis software.

The experiments with water and aqueous solutions were performed in air pre-saturated with the vapour of the liquid and the one with ethylene glycol and glycerol at $50 \pm 3\%$ relative humidity. The measurements were carried out at room temperature, with temperature stability during each experiment maintained within $\pm 0.1°$. The same surfaces were normally used for several experiments. Between each experiment they were rinsed with ethanol and Millipore™ water and blown dry. Complete wetting does not occur for any of the liquids studied in this work.

The aqueous solution of ethanol used in the experiments was always prepared as a 70/30 volume percent EtOH/water mixture.

The surfactant used in the study of dynamic spreading effects was a non-ionic polyethylene glycol alkyl ether, with fourteen carbon atoms in the chain and six ethylene oxide monomer units in the head-group, $C_{14}E_6$. This surfactant was purchased from Nikko Chemicals and was used without further purification. It has the cmc of 1.0×10^{-5} mol l^{-1} [31].

3. Results and discussion

3.1. Spreading behaviour of liquids and water–ethanol solutions

The results presented in this section show principal trends in spreading behaviour of liquids with varying viscosity and surface tension. Fig. 1 shows the time-evolution of the drop contour of a water drop impacting with a hydrophobized glass surface. The drop was released from a height of 1.3 mm above the solid surface. The velocity of the falling drop just before impact was about 0.2 m s^{-1}. The inertia contribution to the drop acceleration is in this case relatively small, but still clearly influencing the initial spreading rate (com-

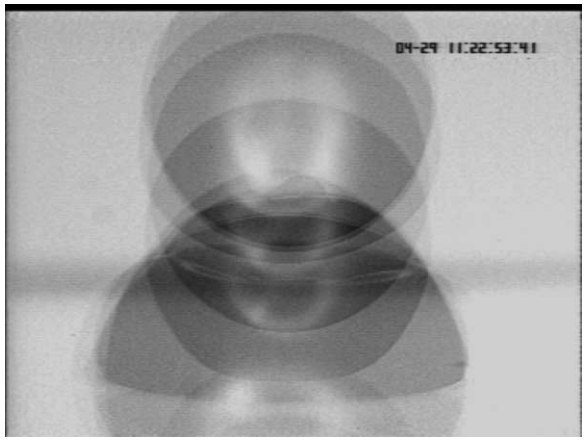

Fig. 1. A water drop is released from a height of 1.3 mm above the substrate and with a velocity of about 0.2 m s^{-1} just before impact. The frequency of the stroboscope was 250 Hz.

pare the spreading rates in Fig. 1 with the rates in Fig. 2). Nevertheless, the impact energy is not sufficient large for the drop to spread much further than the limitations set by the balance of surface and wetting tension forces balance (taking into account hysteresis effects). However, a small tendency to oscillations at tlc can be seen in Fig. 1.

The primary aim of the present study was to study the spreading in the capillary regime, where inertia and gravity effects are small. Therefore,

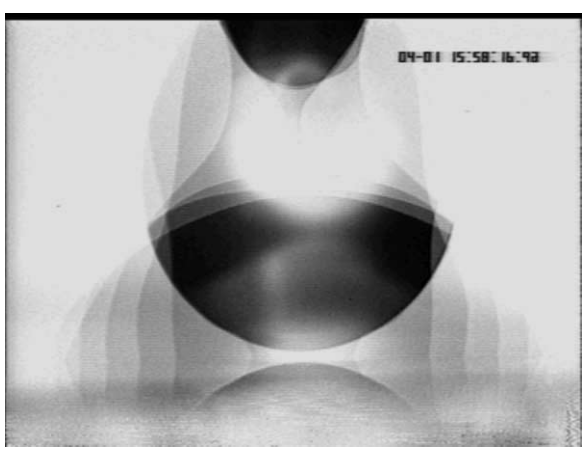

Fig. 2. A water drop is gently deposit on the surface and is therefore ripped off from the syringe by adhesion. The frequency of the stroboscope was 250 Hz.

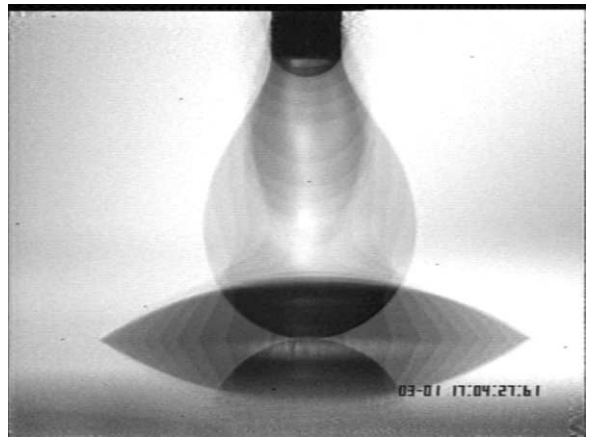

Fig. 3. A drop of a 70/30% EtOH/water mixture is gently deposit on the surface. The frequency of the stroboscope was 570 Hz.

the spreading was studied in situations where the drops were gently contacted with the surface, as schematically seen in Fig. 2. In these experiments, the drop is contacted with the surface while still in contact with the capillary orifice when the spreading process begins. The neck connected to the orifice narrows during the spreading process and the drop is generally ripped off at some intermediate stage of the spreading process. In a few cases, the rip-off was observed to result in a discontinuity in the spreading curve, but generally the effect of the rip-off was not insignificant.

An example showing the spreading behaviour of a water drop contacted gently with the solid surface is shown in Fig. 2. The initial spreading rate is reduced compared to that observed for the falling drop. However, the spreading process is fast, also in this case. Contact angle and drop base values stop changing within about 20 ms. Fig. 3 shows the spreading behaviour on the same kind of substrate of a 70/30% EtOH/water drop. The initial spreading rate of this solution and the time to reach steady values are more or less equal to that observed for water in Fig. 2. However, this corresponds to a larger decrease in the contact angle due to the smaller drop volume. For making comparisons between different systems easier, we chose to normalise the drop base radius (r_b) with the radius the drops had just before contact with

the solid surface. Fig. 4 shows the dependence of the normalised radius (r_n) on time for various liquids and solutions. For the low viscosity water-borne systems, the spreading process is quite fast. The drop radius exhibits an approximate $r_n \sim t^{1/2}$ spreading law. On exiting this regime, the spreading is observed to abruptly reach a halt. Quasi-static conditions are reached in less than 30 ms, showing that the capillary break is effective as equilibrium conditions are approached or slightly surpassed. For comparison, was also show in Fig. 5 some related spreading data obtained for water by Thoroddsen et al. [32]. The experimental data are low impact spreading results from this study exhibiting very much the same spreading behaviour as is observed in the present work. For high impact situations, the spreading versus time deviates from the $\sim t^{1/2}$ spreading law. This behaviour is discussed in a recent study by Gu et al. [33].

The more viscous ethylene glycol and glycerol show a weaker time-dependence. The drop spreading of the viscous glycerol exhibited an approximate $r_n \sim t^{1/10}$ law in the long-time spreading regime, in agreement with earlier theoretical and experimental results [9]. As in most spreading studies, however, the power law relation obtained depends on the time interval chosen to fit the curve.

Nevertheless, for the glycerol and ethylene glycol, our results agree reasonably well with recent findings by de Ruijter et al. [9]. They showed that several different spreading regimes are expected and observed experimentally depending on the time after drop-surface contact. In the initial 'early-time' spreading regime, they predicted that the radius should increase linearly with time. In the second regime, the time-dependence followed predictions of the molecular kinetic theory and, finally, in the asymptotic long-time regime,

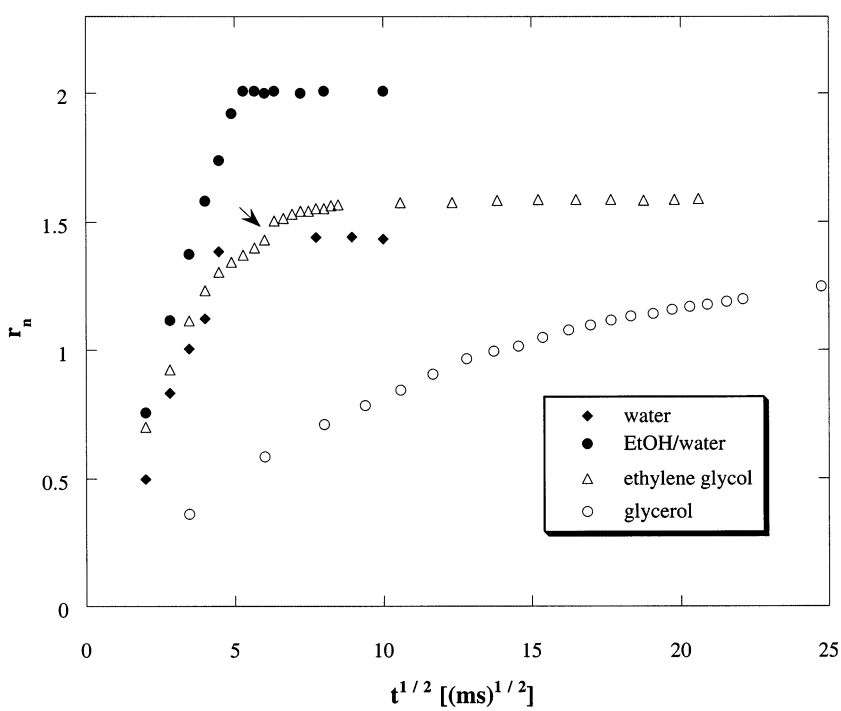

Fig. 4. Normalised radius versus square root of time measured during spreading of different liquids and a 30/70 mixture of EtOH/water on a hydrophobized glass surface. The volumes of the drops varied between 10 and 16 μl and in all this measurements the drops were gently deposited on the surface. The arrow shows for ethylene glycol the time when the drop is detached from the capillary orifice.

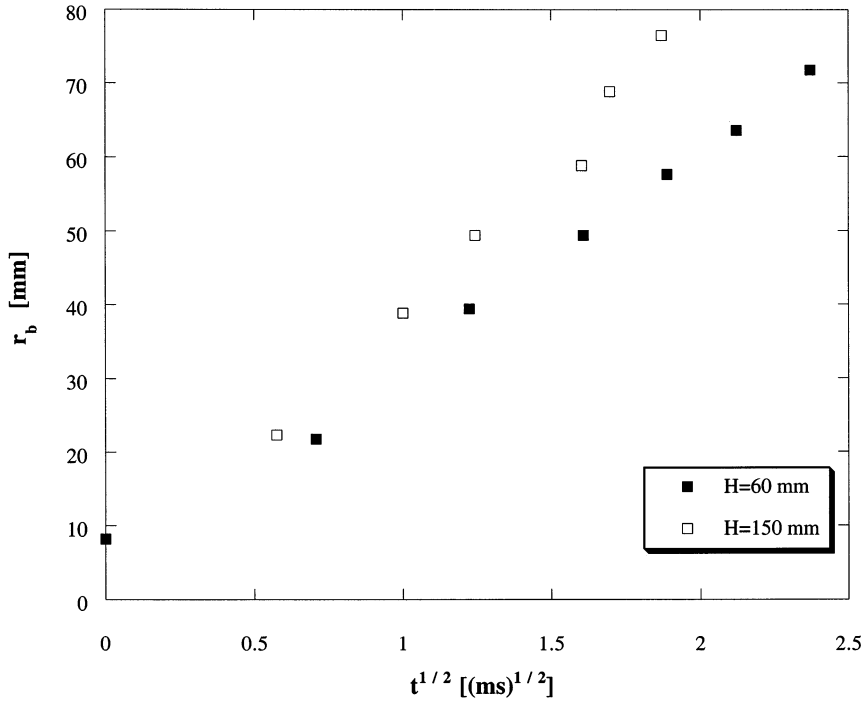

Fig. 5. Drop base radii plotted vs. square root of time for water drops (drop diameter = 5.5 mm, $\gamma_{LV} = 60$ mN m^{-1}) released from different heights (H) above an anodized aluminium surface. The experimental spreading data is from Ref. [32].

spreading followed predictions by the hydrodynamic theory. Finally, they observe a long-time relaxation regime when the drop approaches the equilibrium shape. The crossover time between the two different models mentioned above depends on the drop volume, the strength of the interactions between the surface and the liquid and the viscosity of the liquid. With some good will, the same spreading regimes could be identified in this study for the liquids of high viscosity. However, we chose not to discuss this further and instead focus on the spreading behaviour observed for the water-borne systems.

The main question being the reason for the fast spreading and relatively high power in the apparent spreading law. As already mentioned, r_n increases proportional to $t^{1/2}$ for the low viscous water-borne systems until the base area of the droplet has reached a point where the spreading comes to an abrupt halt. Fig. 6 show typical base area versus the time curves for different EtOH/water drops, verifying this statement. It is seen from the good fits of the base area versus time in this graph that the $r_b \sim t^{1/2}$ spreading law holds for repeated drop spreading measurements and that the drop volume effect on spreading is small. This behaviour is clearly very different from that observed for the high viscous glycerol. It is tempting to attribute the observed spreading behaviour to inertia or gravity effects associated with the contacting of the drop with the solid surface. The gentle mode of contact, the small drop sizes studied, and the fact that the drop is still attached at the capillary orifice in the initial spreading phase do, however, point to the fact that capillary forces should still play a significant role in the spreading.

The bond number of spreading (B) can be used to show the relative magnitude of gravity to capillarity on the spreading process [34].

$$B = \rho g r_b^2 / \gamma_{LV}, \quad (6)$$

where ρ is the liquid density, γ_{LV} is the liquid surface tension, g is the gravity acceleration and r_b is the base radius of the spreading drop. When

$B = 0$ the drop spreading is entirely governed by capillarity and the free-surface shape has the form of a spherical cap. As B increases the gravity force squashes the drop in the vertical direction and the drop profile will be flattened. This is particularly obvious in the initial stage of spreading [35]. In our experiments, the bond number during the spreading process range from 0.05 to less than 1, except for the EtOH/water case and the bigger drops of ethylene glycol. In these two cases the bond numbers are somewhat higher than one at the end of the spreading processes. This indicates clearly that capillarity is important if not dominant.

Furthermore, the out of balance capillary forces (F_c) for the spreading processes were calculated for some spreading drop and meniscus rise measurements by the equation [36]:

$$F_c = \gamma_{LV}(\cos\theta(\infty) - \cos\theta(t)). \quad (7)$$

In the meniscus rise measurements, the meniscus height was studied on a hydrophobic glass rod after contact with an EtOH/water mixture. Fig. 7 displays $\Delta r_b/\Delta t$ between two consecutive flashes or images versus the out of balance capillary force. In the meniscus rise case the change in height of the meniscus (Δh_m) is divided by the time interval. There is a correlation between the two parameters, although the scatter is quite large. Effects of gravity are, however, also seen. In the spreading drop situation, gravity acts in the same direction as the spreading progress and thereby increases the spreading rate. In the meniscus rise experiment gravity plays its dominant role in the end of the spreading process and prevents the spreading. Therefore, the achieved spreading rate is slightly lower in the meniscus rise experiment compared to the spreading drop.

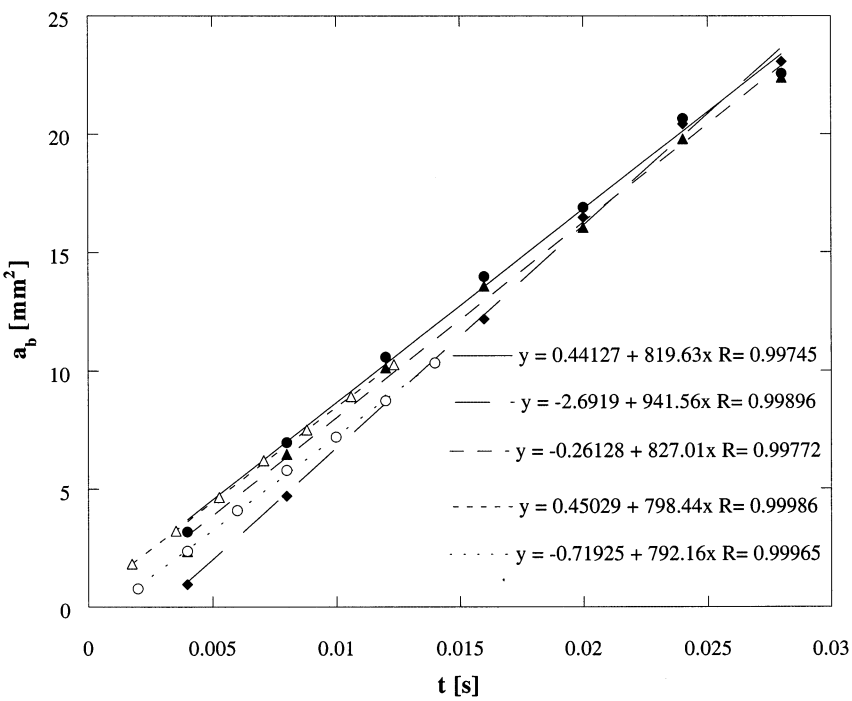

Fig. 6. Drop base area (a_b) versus time curves for the EtOH/water drops. Filled markers show data obtained for 10 μl drops, while unfilled marker show the corresponding spreading for 5 μl drops.

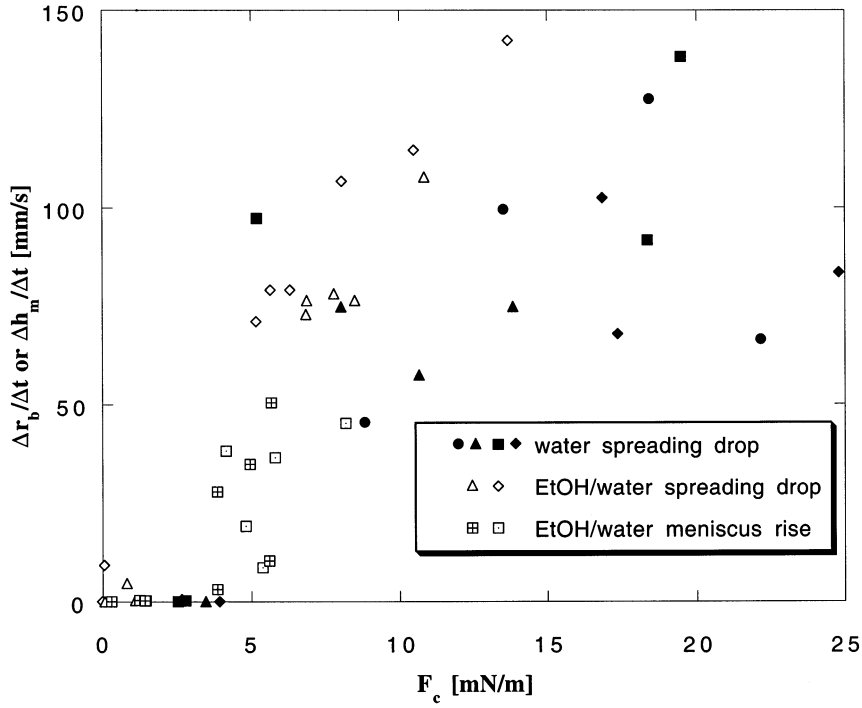

Fig. 7. $\Delta r_b/\Delta t$ between two consecutive flashes or images plotted versus the out of balance capillary force. In the meniscus rise case, the change in height of the meniscus (Δh_m) is divided by the time interval.

3.2. Influence of surface-active additives

The surface tension relaxation times for the EtOH/water solution are very fast compared to the drop spreading dynamics. Fig. 4 confirms that this solution should spread as pure liquid in saturated atmosphere when evaporation effects are negligible. Solutions with low concentrations of surfactant, on the other hand, exhibit surface tension decay rates comparable to or even slower than the expansion rates of the drop interfaces during spreading. For such solutions, we observe a two step spreading process, Fig. 8. In the first phase, the spreading of the pre-equilibrated surfactant drop is reminiscent of that of pure liquid water or the EtOH/water mixture. The breakpoint where the rapid spreading halts is intermediate to that observed for pure water and EtOH/water, respectively (Fig. 8). Hence, pre-adsorbed surfactant at the lv interface aids spreading in the short-time spreading regime. This clearly shows that the three-phase transfer rate from the *lv* to the *ls* interface is rapid compared to the spreading rate in this region. However, as the *lv* and *ls* interfaces expand, the surface concentration of surfactant is reduced and the surface tension increases. This explains the fact that the radius where spreading is observed to halt, is intermediate to that of water and the EtOH/water mixture, despite the fact that the equilibrium surface tension of the surfactant solution is more or less the same as for the EtOH/water mixture. For the latter case, the adsorption rate from the bulk to the *lv* and *ls* interfaces is rapid enough so that a constant surface tension is kept constant during the whole spreading process. In Fig. 8, we also show the spreading of a surfactant drop that is freshly formed at the solid surface. In contrast to the pre-equilibrated drop this spreads to a lesser degree in the fast spreading regime. This is clearly due to the higher initial surface tension in absence of pre-adsorbed surfactant. The drops are identical in composition, but have a different partitioning of surfactant molecules between the *lv*

interface and the bulk at the start of the spreading process.

Fig. 8 shows for both surfactant solutions that the final radius achieved after the slow relaxation of the drop spreading is equal to that obtained after the rapid initial spreading phase for the EtOH/water mixture. This slow second spreading phase reflects the adsorption process from the bulk to the expanding *lv* interface and the associated surface tension relaxation. Perhaps more correctly for the pre-equilibrated system, it reflects the re-adsorption to this due to spreading depleted interface. Since we know that the hydrostatic equilibrium is reached quickly for these low viscosity drops and that the transfer rate across the TCL is also rapid, the spreading dynamics can in this regime in terms of the dynamic contact angle be approximated as:

$$\cos\theta(t) = \frac{\gamma_{sv} - \gamma_{sl}}{\gamma_{lv}(t)}, \tag{9}$$

where the γ_{sv} interfacial tension is assumed constant due to principal lack of surfactant adsorption driving force to this interface bordering air and the hydrophobic surface. In terms of the drop radius, this condition for a hemispherical can be written as

$$r_b(t) = \left(\frac{3V}{\pi} P(\theta(t))\right)^{1/3}, \tag{10}$$

where

$$P(\theta(t)) = \frac{\sin^3\theta(t)}{2 - 3\cos\theta(t) + \cos^3\theta(t)}, \tag{11}$$

Hence, the spreading rate of surfactant solutions on hydrophobic surfaces may quite simply be approximated from dynamic surface tension data by using Eqs. (9)–(11). For accurate predictions, this require taking into account the expansion of the *lv* and *ls* interfaces as well as the value of adsorption reached prior to contact with the solid surface that depends on the drop history.

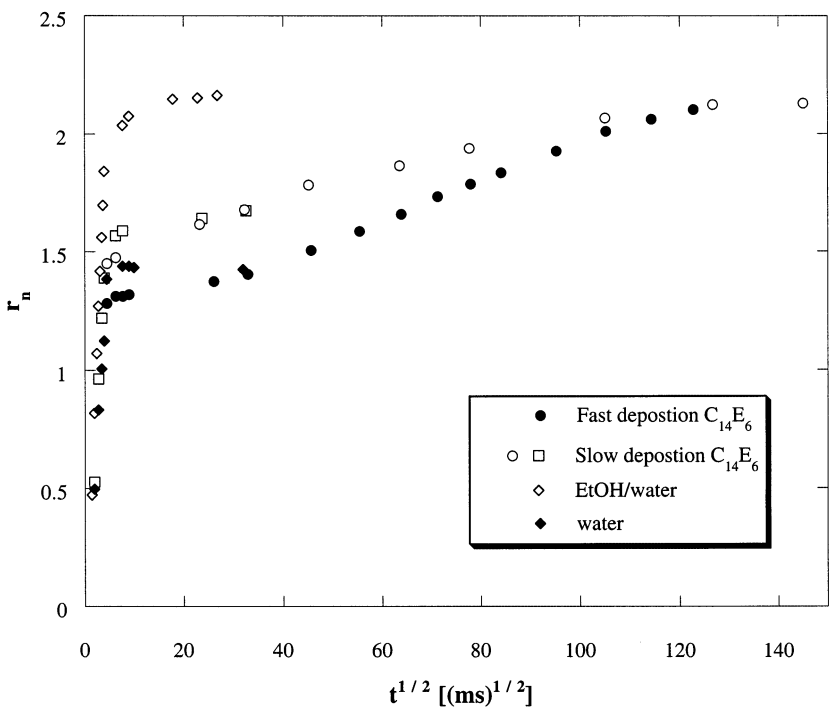

Fig. 8. Normalised radius versus square root of spreading time for drops of water, EtOH/water mixture and a 0.2 mM $C_{14}E_6$ solution. The drop surface tension was allowed to equilibrate before contact with the solid surface in the slow deposition mode, whereas the drop was ejected directly on the surface in the fast deposition mode. The time of drop formation was in the latter case about 50 ms. The analysis of the images in this case started after 60 ms.

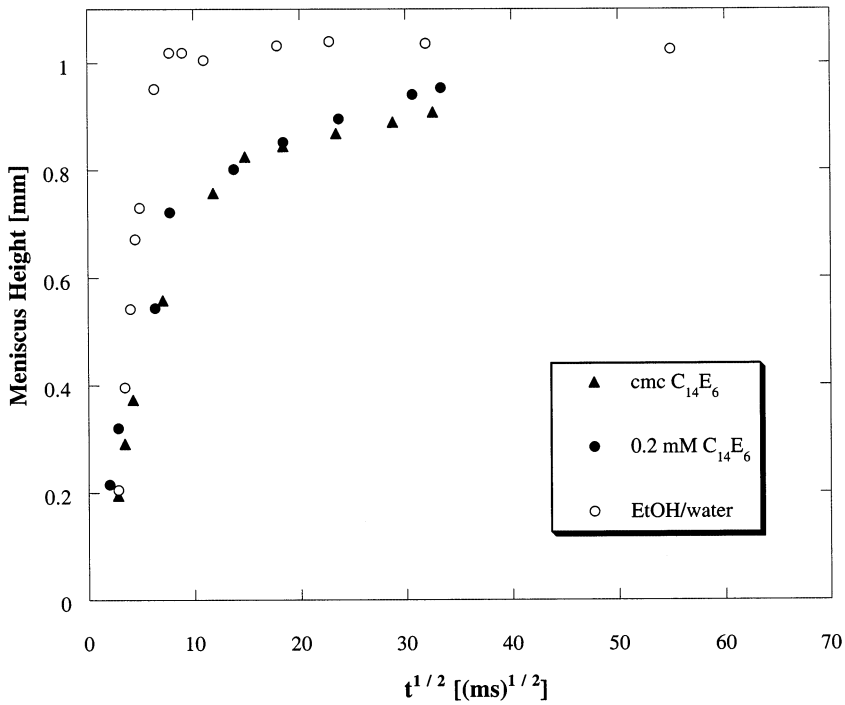

Fig. 9. Shows the meniscus rise on the rod as a function of the square root of time. The rod was immediately stopped when it hit the liquid surface.

It should be noted that applicability of Eq. (9) is limited to a specific case where adsorption to the *sl* interface does not change with time. Under certain conditions, which often apply to the spreading of small drops of surfactant solutions over hydrophobic substrates, the accumulation of surfactant at the solid/liquid interface is effected by transfer of surfactants over the TCL [37]. The amount, Γ_{sl}, of surfactant adsorbed to the solid/liquid interface changes with time, t, according to the following equation [37]:

$$\Gamma_{sl}(t) = \Gamma_{sl}^{m}\left\{1 - \exp\left(-\frac{k_{sl}^{+}\Gamma_{lv}(t)}{v\Gamma_{sl}^{m}}\right)\right\} \quad (12)$$

that relates the adsorption to the sl interface to the surface excess, Γ_{lv}, of surfactant at the *lv* interface. Here, Γ_{sl}^{m} is the monolayer adsorption capacity, v is the velocity of advancing liquid front, and k_{sl}^{+} is the three-phase line transfer rate constant. If k_{sl}^{+} is large, the amount of surfactant adsorbed to the *sl* interface is essentially constant and equals Γ_{sl}^{m}. If this is the case, as was tacitly assumed a previous paper [37], the corresponding surface tension component, γ_{sl}, is constant as well. In the opposite limit, when k_{sl}^{+} is small, $\Gamma_{sl}(t)$ appears to be proportional to $\Gamma_{lv}(t)$, and hence, γ_{sl} becomes time-dependent, being covariant with γ_{lv}. Therefore, the actual changes in the contact angle may be greater than predicted by Eq. (9).

The noteworthy observation in Fig. 8 is that the drop base after the initial spreading phase appears to halt for a short period of time. This may be related to the fact that the force balance at this stage is close to equilibrium. For further spreading to occur, a critical wetting tension must be built-up for the three-phase line to overcome hysteresis that may pin the contact line. This critical wetting tension will be overcome through adsorption at the *lv* interface and subsequent TCL transfer of surfactant to the *ls* interface, whereby the wetting tension is increased.

Fig. 9 shows the same measurement as in Fig. 8, but instead of drop spreading the meniscus rise on hydrophobic glass rod has been studied after

contact with a surfactant solution or a EtOH/water mixture. As can be seen in Fig. 9, the initial meniscus rise is rapid for the EtOH/water mixture as well as for the surfactant solutions. However, for the surfactant solutions the speed of the meniscus rise is retarded at the end of the spreading process. For the EtOH/water mixture, the fast adsorption from the concentrated solution and the likewise high three-phase line transfer rates keeps the capillary force more or less constant from the moment the liquid touches the rod until the static-state rise condition is reached. In the dilute surfactant solutions, the slower surface diffusion and three-phase line adsorption rates from the bulk limits the spreading rate on the rod when the *lv* interface becomes depleted. Due to the relatively speaking much larger *lv* interface in the rod experiment, and therefore also a much larger surfactant reservoir at this interface as compared with the drop experiment, the rates of surface diffusion at the *lv* interface control the rate of the spreading and rise on the rod. The much slower diffusion controlled adsorption process is hence not controlling the spreading rates on the rod as was observed in the later drop spreading stages. This is proven by the fact that the dynamics of the surfactant solution spreading is more or less the same for the 0.01 and 0.2 mM surfactant solution, respectively, despite the fact that bulk adsorption rates and concomitant surface tension decay differ strongly for these two solutions [38,39]. From the spreading data in Fig. 9, one could indeed approximate the surface diffusion rates by assuming that the three-phase line is a perfect sink.

The slower surfactant solution spreading in the drop experiments compared to in the rod experiments is explained by the necessity of supplying the *ls* interface with surfactant via *lv* adsorption from the bulk solution which is a slow process according to the low bulk surfactant concentration in the bulk. Furthermore, in the spreading drop case at low surfactant concentration, the large interfacial expansion-to-bulk volume ratio will result in a depletion of the bulk solution, which will further decrease the rate of spreading. This depletion effect is also the explanation to why no spreading is observed for drops at cmc for $C_{14}E_6$ solution [39].

Acknowledgements

The Swedish Pulp and Paper Research Foundation and the Paper Surfaces for Digital Printing Programme are acknowledged for the financial support.

References

[1] A.W. Adamson, A.P. Gast, Physical Chemistry of Surfaces, Wiley, New York, 1997.
[2] P.G. de Gennes, Rev. Mod. Phys. 57 (1985) 827.
[3] R.G. Cox, J. Fluid. Mech. 168 (1986) 169.
[4] O.V. Voinov, Fluid Dynam. 11 (1976) 714.
[5] S. Gladstone, in: K.J. Laidler, H. Eyring (Eds.), Theory of Rate Processes, McGraw-Hill, New York, 1941.
[6] T.D. Blake, J.M. Haynes, J. Coll. Interf. Sci. 30 (1969) 421.
[7] T.D. Blake, A. Clarke, J. De Coninck, M.J. de Ruijter, Langmuir 13 (1997) 2164.
[8] F. Brochard-Wyart, P.G. de Gennes, Adv. Coll. Interf. Sci. 39 (1992) 1.
[9] M.J. de Ruijter, J. De Coninck, G. Oshanin, Langmuir 15 (1999) 2209.
[10] M.J. de Ruijter, J. De Coninck, T.D. Blake, A. Clarke, A. Rankin, Langmuir 13 (1997) 7293.
[11] M.J. de Ruijter, M. Charlot, M. Voué, J. De Coninck, Langmuir 16 (2000) 2363.
[12] S. Gerdes. Dynamic Wetting of Solid Surfaces Influence of Surface Structure and Surface Active Polymers. Ph.D. thesis, Lund University, 1998.
[13] A. Bose, in: J.C. Berg (Ed.), Wettability, Marcel Dekker, New York, 1993, p. 149.
[14] A.K. Chesters, A.B.A. Elyousfi, J. Coll. Interf. Sci. 207 (1998) 20.
[15] K.P. Ananthapadmanabhan, E.D. Goddard, P. Chandar, Coll. Surf. 44 (1990) 281.
[16] B. Frank, S. Garoff, Coll. Surf. A: Physicochem. Eng. Aspects 116 (1996) 31.
[17] C.S. Gau, G. Zografi, J. Coll. Interf. Sci. 140 (1990) 1.
[18] R.M. Hill, M. He, H.T. Davis, L.E. Scriven, Langmuir 10 (1994) 1724.
[19] R.M. Hill, Curr. Op. Coll. Interf. Sci. 3 (1998) 247.
[20] J.F. Joanny, J. Coll. Interf. Sci. 128 (1989) 407.
[21] Z. Lin, R.M. Hill, H.T. Davis, M.D. Ward, Langmuir 10 (1994)
[22] M.J. Rosen, L.D. Song, Langmuir 12 (1996) 4945.
[23] T. Stoebe, Z. Lin, R.M. Hill, M.D. Ward, H.T. Davis, Langmuir 12 (1996) 337.
[24] T. Stoebe, Z. Lin, R.M. Hill, M.D. Ward, H.T. Davis, Langmuir 13 (1997) 7270.
[25] S. Padmanabhan, A. Bose, J. Coll. Interf. Sci. 126 (1988) 164.

[26] V. Yaminsky, B. Ninham, M. Karaman, Langmuir 13 (1997) 5979.
[27] M. Rein, Fluid Dynam. Res. 12 (1993) 61.
[28] N. Mourougou-Candoni, B. Prunet-Foch, F. Legay, M. Vignes-Adler, K. Wong, J. Coll. Interf. Sci. 192 (1997) 129.
[29] N. Mourougou-Candoni, B. Prunet-Foch, F. Legay, M. Vignes-Adler, Langmuir 15 (1999) 6563.
[30] M. Pasandideh-Fard, Y.M. Qiao, S. Chandra, J. Mostaghimi, Phys. Fluids 8 (1996) 650.
[31] P. Mukerjee, K.J. Mysels, Critical Micelle Concentrations of Aqueous Surfactant Systems, National Standard Reference Data System, National Bureau of Standards (US), Washington, DC, 1971.
[32] S.T. Thoroddsen, J. Sakakibara, Phys. Fluids 10 (1998) 1359.
[33] Y. Gu, D. Li, Coll. Surf. A: Physicochem. Eng. Aspects 163 (2000) 239.
[34] S.F. Kistler, in: J.C. Berg (Ed.), Wettability, Marcel Dekker, New York, 1993, p. 311.
[35] Y.D. Shikhmurzaev, Phys. Fluids 9 (1997) 266.
[36] T.D. Blake, in: J.C. Berg (Ed.), Wettability, Marcel Dekker, New York, 1993, p. 291.
[37] F. Tiberg, B. Zhmud, K. Hallstensson, M. von Bahr, Phys. Chem. Chem. Phys. 2 (2000) 5189.
[38] F. Tiberg, J. Chem. Soc. Faraday Trans. 92 (1996) 531.
[39] M. von Bahr, F. Tiberg, B.V. Zhmud, Langmuir 15 (1999) 7069.